Journal of Polymer Research (2019) 26:207
https://doi.org/10.1007/s10965-019-1852-z

ORIGINAL PAPER

Fluorinated polyimide nanocomposites for low K dielectric applications

S. Kurinchyselvan[1] · A. Hariharan[2] · P. Prabunathan[2] · P. Gomathipriya[1] · M. Alagar[2]

Received: 31 December 2018 / Accepted: 4 July 2019

Abstract

A novel fluorinated amine compound prepared was characterized by ^{1}H NMR, ^{19}F NMR and FTIR. Subsequently, polymerized with pyromellitic dianhydride results in the formation of neat fluorinated polyimide matrix (PI). In addition, three different nanomaterials such as of graphene oxide (GO), Octa (aminophenyl) silsesquioxane (OAPS) and graphene oxide blended with Octa (aminophenyl) silsesquioxane (GO-OAPS) were reinforced separately with PI in varying weight percentages. The developed composites were studied for their thermal, dielectric and hydrophobic behaviour and compared. Comparatively the 7% OAPS-GO/PI exhibits lower dielectric constant (k = 2.1) than that of neat PI, GO/PI and OAPS/PI composites. The OAPS grafted onto the GO surface contributes for lower polarity due to its porous caged structure and contributes for higher insulation behaviour. Further, the 7% OAPS-GO/PI also exhibits higher contact angle (107°) due to the less polar nature of the composites which in turn contributes to enhanced hydrophobic behaviour. The data obtained from morphological, surface and dielectric studies indicate that the OAPS-GO/PI composites exhibited substantially improved hydrophobic and dielectric properties than that of GO/PI and OAPS/PI.

Keywords Polyimide · Bisphenol AF · Octa(aminophenyl) silsesquioxane (OAPS) · Graphene oxide · Hybrid composites · Thermal stability · Contact angle · Dielectric constant

Introduction

The increasing demand for low dielectric materials leads to invention of new materials including polymeric composites. The low dielectric materials find diverse applications as insulator in electronic industry as interlayer dielectrics to reduce the resistance-capacitance time delay, cross talk, and power dissipation [1]. Comparatively, polymer based interlayer dielectric materials (ILD) attracted more attention because of their low cost, easy processability and excellent performance [2]. Polyimides (PIs) have been widely used as dielectric and packaging materials in the microelectronics industry because of their several merits such as good mechanical, thermal and dielectric properties [3–7]. Even though the value of dielectric constant of conventional polyimides are in the wide range from 3.2 to 3.9, the requirement of ILD for ultra-large-scale integration (ULSI) multilevel interconnections does not satisfied yet. Hence, there is still need for more demanding low dielectric polyimide matrices or composites.

In order to achieve low dielectric constant values, several significant modification methods such as the incorporation of fluorine moiety, long aliphatic chain, porous silica materials such as polyhedral oligomeric silsesquioxanes (POSS) derivatives, MCM-41 and SBA-15 have been adopted [8–12]. In addition to reinforcing low dielectric materials, it was found that introduction of fluorine moiety into polyimide structures is also one of the most effective methods to decrease the value of dielectric constant [13]. Due to high electro-negativity and low polarity of fluorine atom, the fluorinated polyimides contribute to a significant characteristics such as low moisture intake, oil repellence, thermal and chemical stability. Hence, it is expected that the fluorinated polyimides will function as an effective ILD materials.

Electronic supplementary material The online version of this article (https://doi.org/10.1007/s10965-019-1852-z) contains supplementary material, which is available to authorized users.

✉ M. Alagar
mkalagar@yahoo.com

[1] Department of Chemical Engineering, Anna University, Chennai 600025, India

[2] Polymer Engineering Laboratory, PSG Institute of Technology and Applied Research, Coimbatore 641 062, India

Published online: 02 August 2019

Scheme 1 Synthesis of BNFP and BAFP

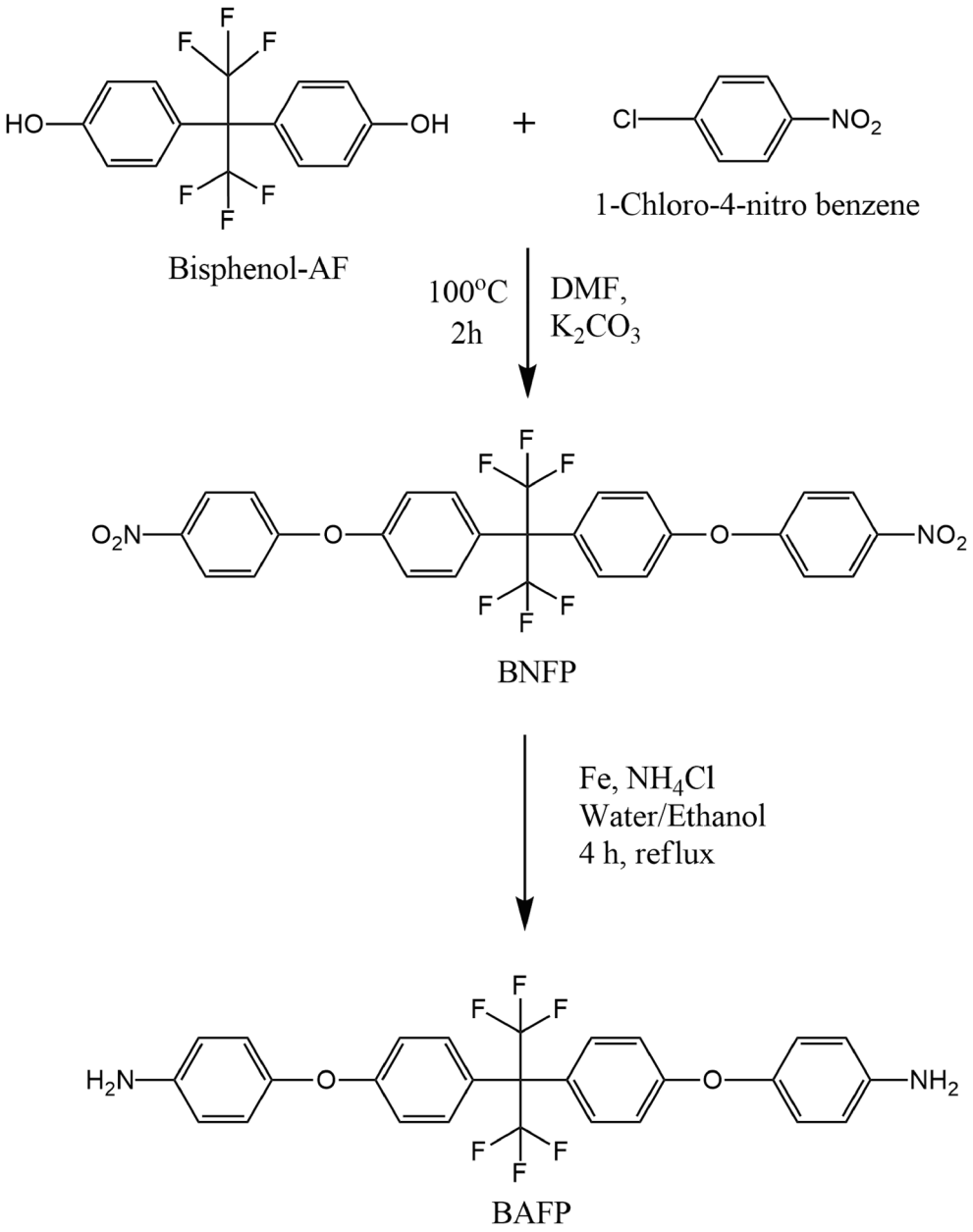

Recently, graphene oxide has great potential to improve the properties of polymers because of it's high aspect ratio, high conductivity, unique graphitized planar structure, and cost competitive process [14–17]. Due to its unique chemical structure with covalently bonded carbon atoms bearing various oxygen functional groups such as hydroxyl, epoxide and carbonyl groups on the basal planes and edges, it can be modified to improve the polymer properties. The oxygen functional groups present on the GO surface provide electrical insulation and versatile sites for chemical functionalization, improving the compatibility, and enhancing the dispersion of GO in polymeric matrices [18–20]. Further, its layered arrangement offers lamellar structure, which could able to reduce the polarization and lower the value of dielectric constant.

Polyhedral oligomeric silsesquioxane (POSS) is important reinforcing nanomaterial in the field of advanced polymeric composites, due to its unique cage like molecular structure and physicochemical properties. Silsesquioxanes are nanostructured materials having inorganic silicon and oxygen molecules externally surrounded by organic molecules and represented by the formula $(RSiO_{1.5})_n$, where R represents hydrogen atom or various functionalized groups like alkyl, alkene, hydroxyl or epoxide unit. POSS cages consist of Si − O inorganic bonds, Si atoms at the eight top angles of the cube structure bridging with O atoms, and eight substitutive groups R on the Si atom. An incorporation of POSS as reinforcing material in the polymer composite system significantly enhances the properties like thermal, mechanical and more importantly lowers the value of dielectric constant [21–26].

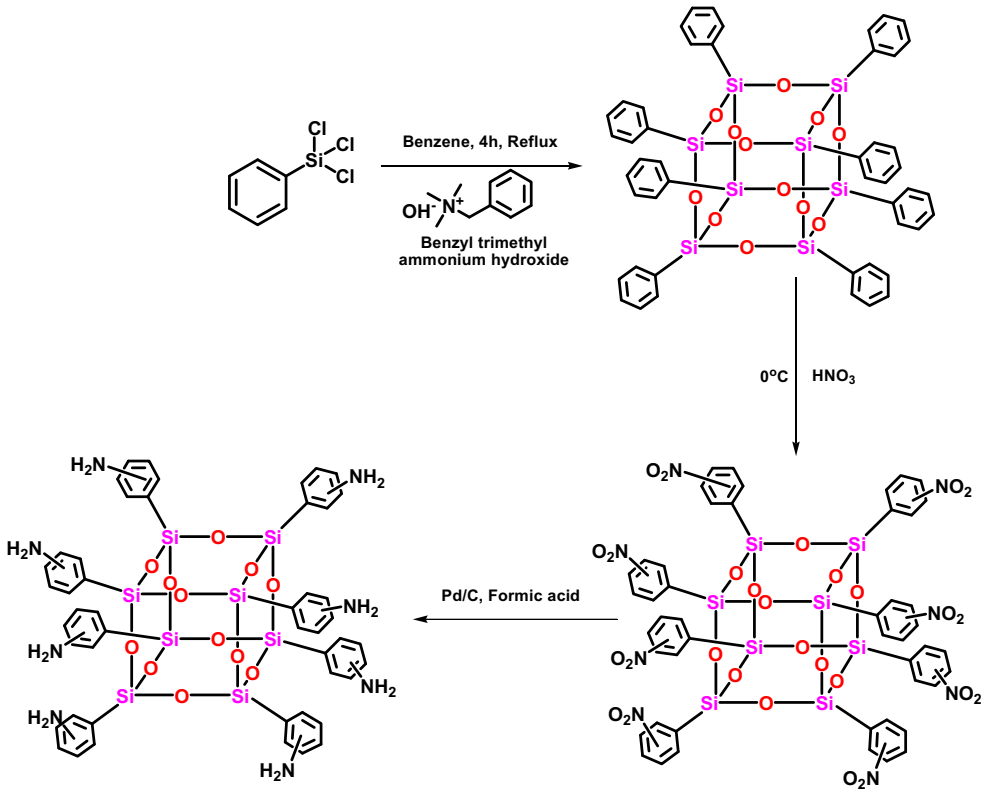

Scheme 2 Synthesis of Octa(aminophenyl)silsesquioxane (OAPS)

Scheme 3 Synthesis of octa(aminophenyl) silsesquioxane (OAPS) and OAPS-GO

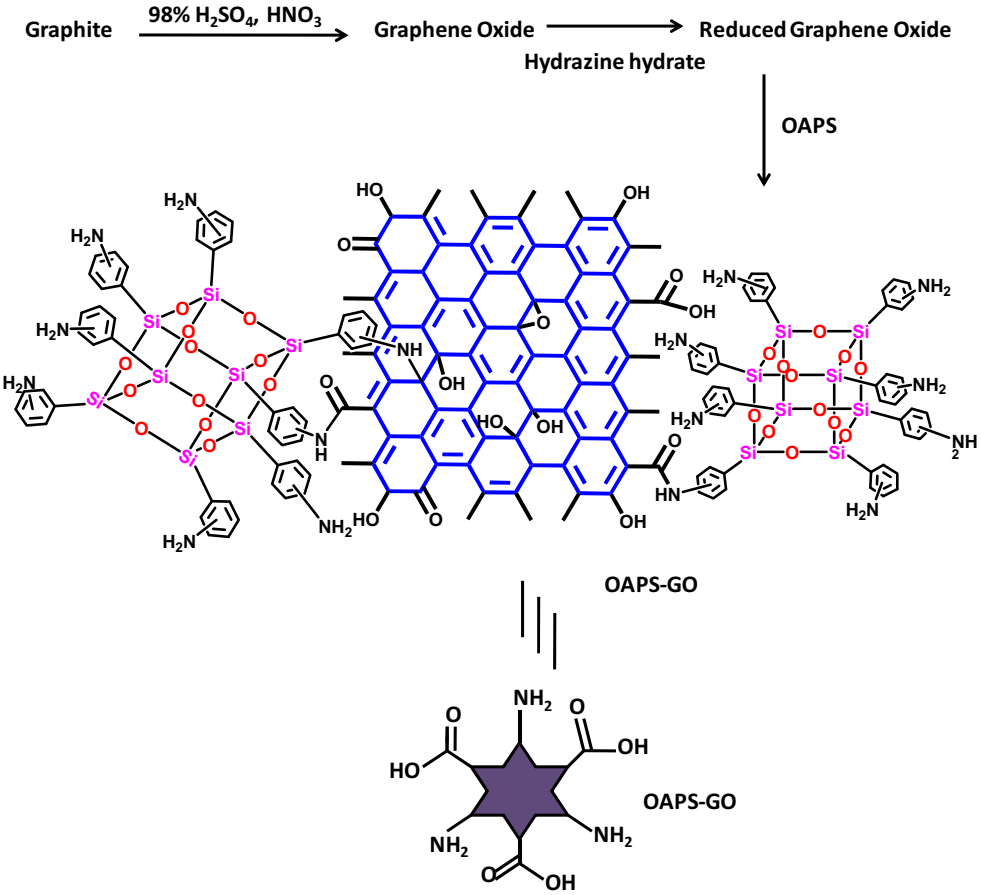

Scheme 4 Preparation of neat polyimide (neat PI)

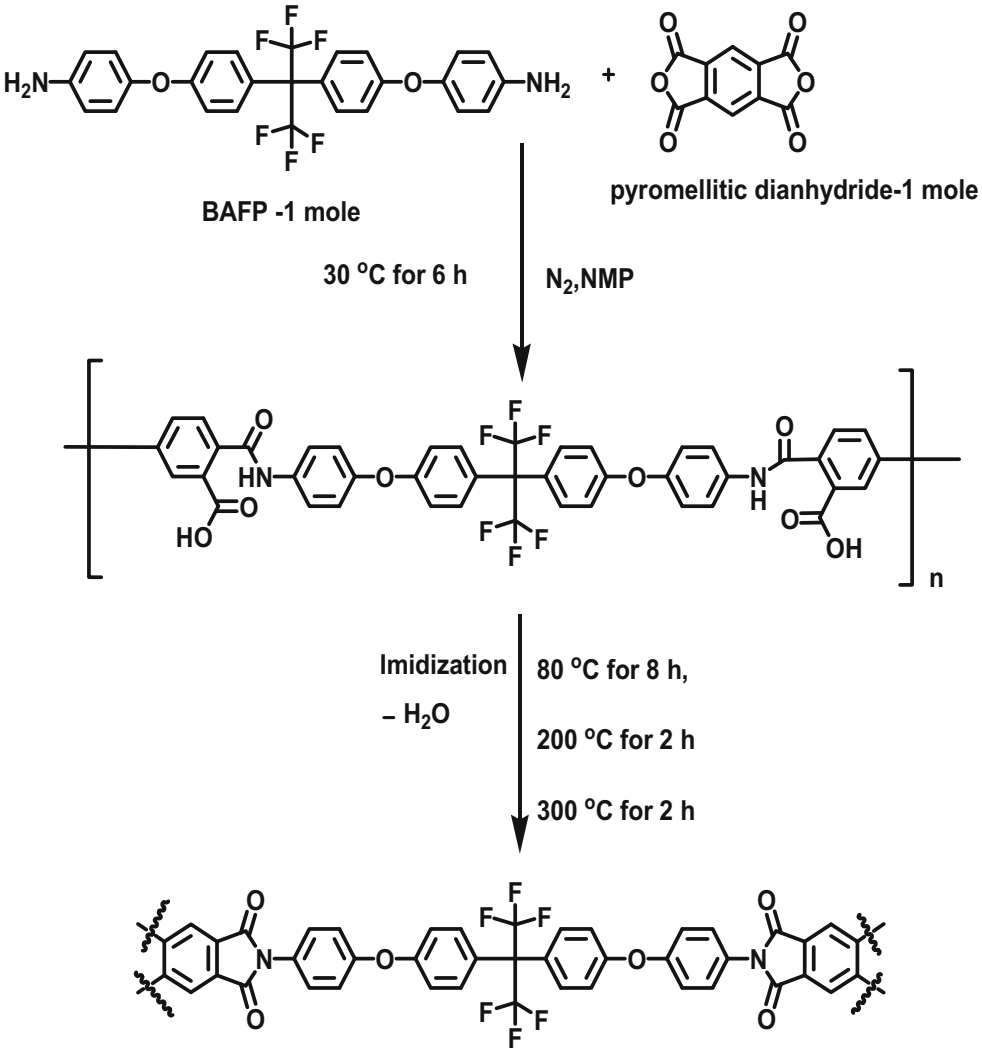

Thus, in the present work an attempt has been made to prepare fluorine containing polyimide based composites using reinforced with three different reinforcing nanomaterials such as of graphene oxide (GO), graphene oxide blended with Octa (aminophenyl) silsesquioxane (GO-OAPS) and OAPS in varying weight percentages. The developed composites were studied for their thermal, dielectric and hydrophobic behaviour. Since, the presence of fluorine not only reduces the value of dielectric constant but also improves the hydrophobic behaviour. Data resulted from different studies are discussed and reported.

Experimental

Materials

Analytical grades of 1-chloro-4-nitrobenzene, potassium carbonate (K_2CO_3), ethanol, ethyl acetate, chloroform, benzene, tetrahydrofuron (THF), N-methyl-2-pyrrolidone (NMP), N, N-dimethylformamide (DMF), sodium hydroxide (NaOH) were procured from SRL chemicals, India. Iron powder, ammonium chloride (NH_4Cl), sodium sulfate (Na_2SO_4) were obtained from Qualigens fine chemicals pvt. ltd, India. Bisphenol–AF, Phenyltrichlorosilane, benzyl trimethylammonium hydroxide, 10 wt% Pd/C, PMDA, graphite were purchased from Sigma Aldrich, Bangalore India.

Synthesis of BNFP

Bisphenol–AF (4, 4-(Hexafluoro iso propylidene) diphenol) (30 g, 0.0892 mol) and 1-chloro-4-nitrobenzene (0.1784 mol) were first dissolved in 240 mL of N, N-dimethylformamide (DMF) in a 500-mL round bottomed flask with constant stirring. Potassium carbonate (0.2676 mol) was added subsequently and allowed to reflux for 12 h. The obtained product was poured into an ice water and the resulting pale yellow solid precipitate (BNFP) was filtered with ice water washing and then dried under vacuum at 100°*C* (Scheme 1).

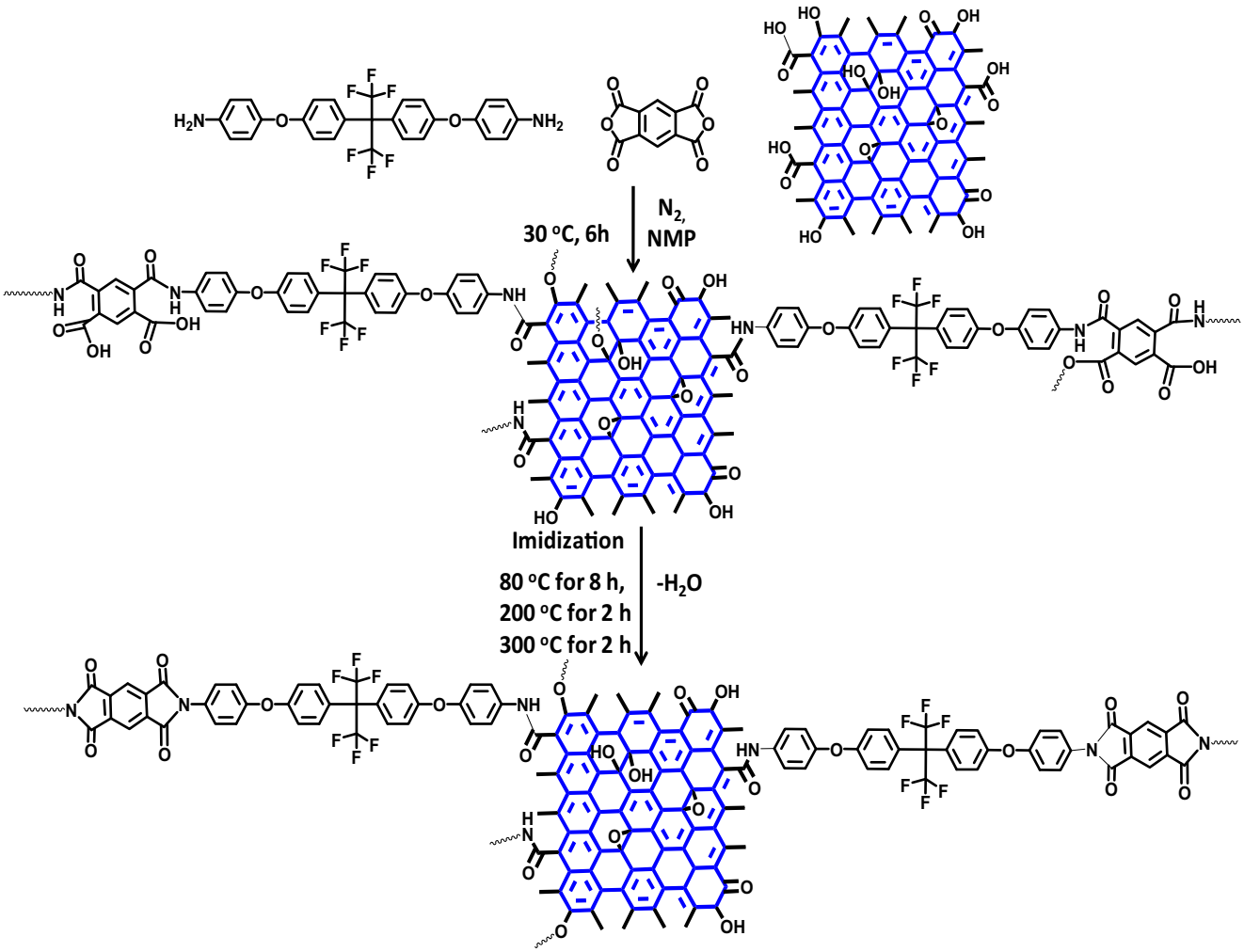

Scheme 5 Preparation of PI Nanocomposites with GO

Synthesis of BAFP

To a suspension of 2,2-bis(4-(4-nitrophenoxy)phenyl)-1,1,1,3,3,3-hexafluoropropane (BNFP) and iron powder (0.3108 mol) in ethanol (10 volume), a solution of ammonium chloride (0.2072 mol) in water (2 volume) were added at 10 °*C* and the allowed to reflux for 4 h. After the completion of reaction, the reaction product was cooled to room temperature and quenched in ice water. Subsequently, an excess amount of chloroform was added and filtered through celite bed. Then the filtrate was extracted using chloroform and washed with sodium bicarbonate, water, and finally with brine solution. Then the organic portion was concentrated under reduced pressure to obtain the product BAFP. The yield was 75% (Scheme 1).

Preparation of graphene oxide (GO)

Graphene oxide was prepared from natural graphite by the process of modified Hummers method using a mixture of sodium nitrate, sulfuric acid, and potassium permanganate. To a suspended solution of natural graphite (10 g) in concentrated sulfuric acid in an ice bath at about 0 °C, sodium nitrate (5 g) was added gradually and stirred for 10 min. Followed by, potassium permanganate was added slowly to the reaction mixture at the same temperature. Then the solution was oxidized by thermal process, and the temperature was maintained at about 40 °C for 24 h. After that, distilled water was added slowly to the reaction mixture under the controlled temperature of about below 100 °C. Subsequently, 30% hydrogen peroxide and excess amount of distilled water were added for the termination of reaction and obtained precipitate was centrifuged and washed several times with water until the pH became 7 and dried in a vacuum oven at 70 °C.

Synthesis of Octaphenylsilsesquioxane (OPS)

Phenyltrichlorosilane (132.25 g, 100 mL, 0.625 mol.) was placed, along with benzene (630 mL), in a three-necked round-bottomed flask fitted with a magnetic stirrer and a

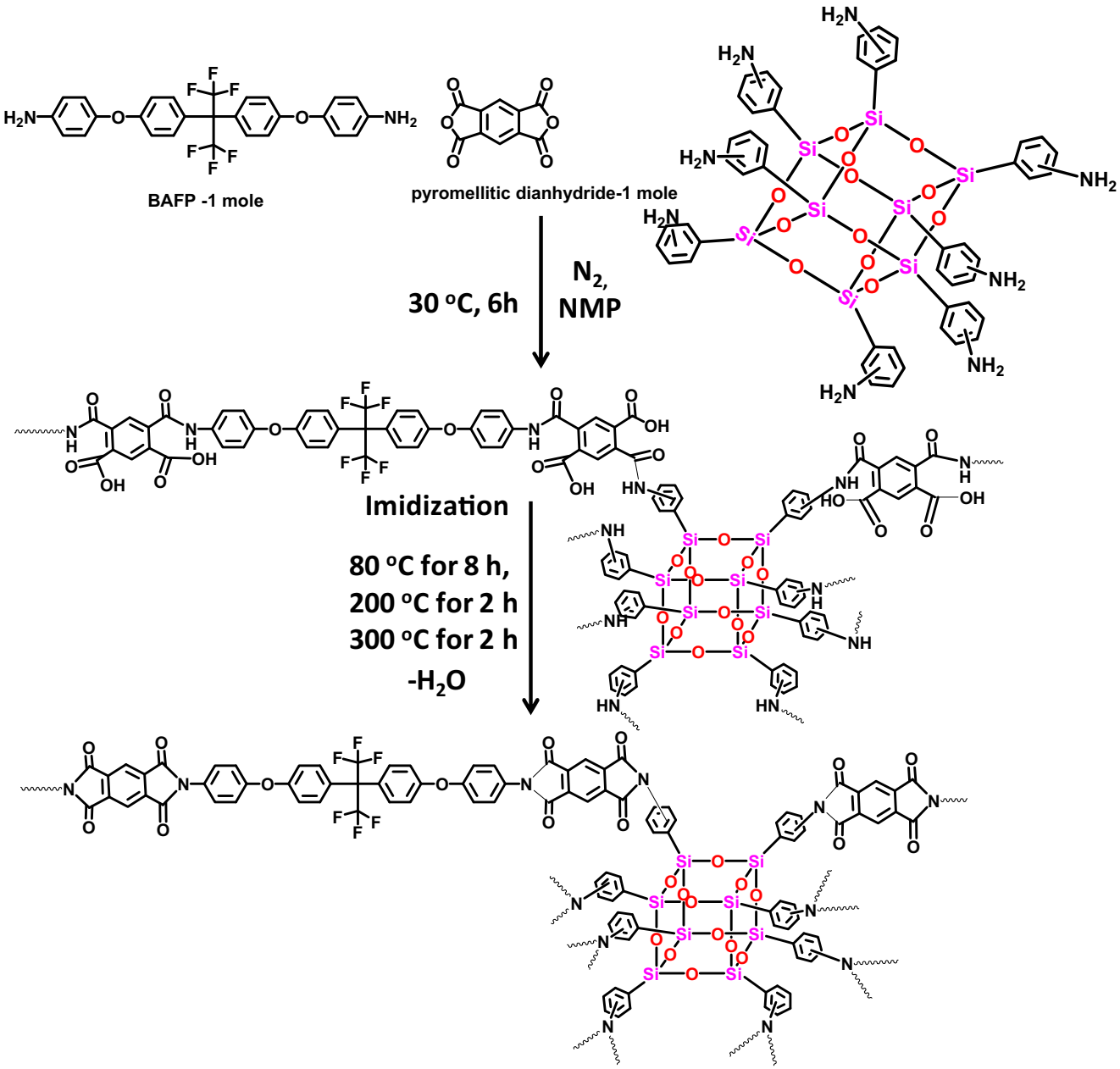

Scheme 6 Preparation of PI Nanocomposites with OAPS

dropping funnel. The reaction was carried out at 25°*C* with addition of water (330 g) slowly and constantly agitated for 12 h. Then the reaction mixture was washed with water until it became neutral, and the aqueous layer was removed. To the organic layer methanolic benzyl trimethylammonium hydroxide (40%, 17 mL) was added and refluxed for 4 h. The reaction mixture was allowed to stand at 25°*C* for 4 days and was further refluxed for 24 h and then cooled and filtered to obtain a white powder. The product (OPS) obtained was extracted using dry benzene in a Soxhlet extractor to remove the soluble resin if any and further dried in vacuum at 70 °C. The yield: 73.5 g (91%).

Synthesis of Octa (nitrophenyl) silsesquioxane (ONPS)

ONPS was synthesized by adopting a procedure reported elsewhere [27]. Fuming nitric acid (360 mL) was placed in a three-necked, round-bottomed flask, equipped with a mechanical stirrer, and the flask was cooled in an ice bath before OPS (60 g) was added portion wise. The resulting mixture was kept in an ice cold condition for an hour with constant agitation for 12 h at 25°*C*. Then the reaction mixture was poured on to ice, and the light yellow precipitate obtained was removed by filtration, washed with deionized water until neutral pH was obtained, and then washed twice with ethanol (2 × 120 mL). The solid product

Scheme 7 Preparation of PI Nanocomposites with GO-OAPS

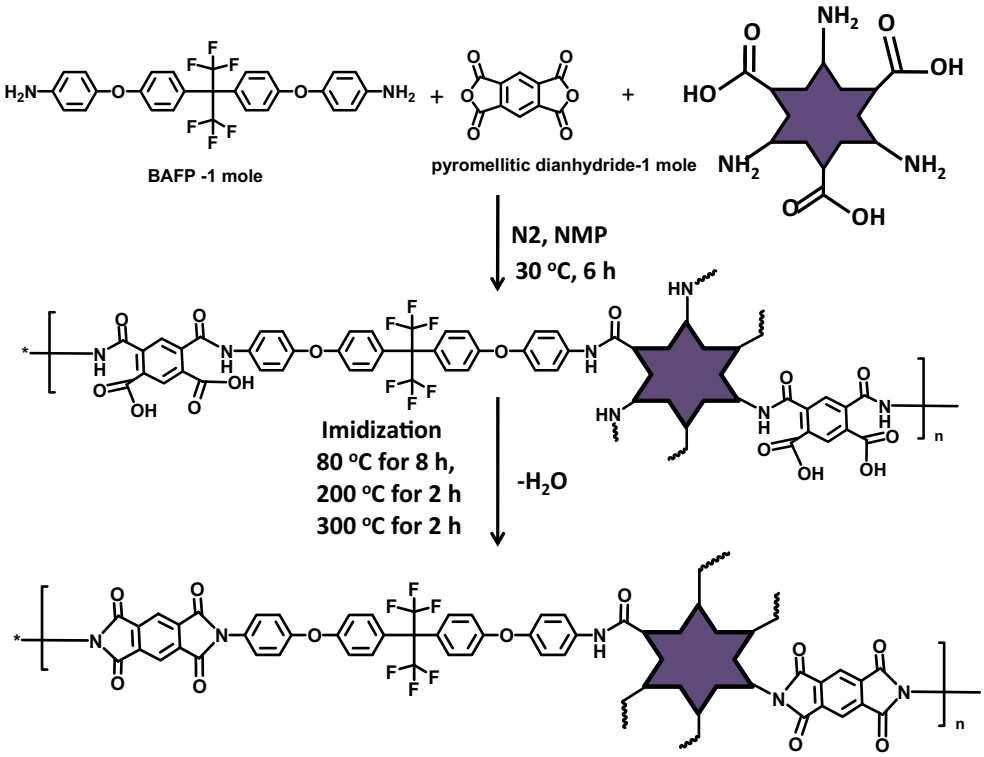

(octa(nitrophenyl) silsesquioxane) obtained (Scheme 2) was air-dried at 25 °C for 12 h. Yield: 72.0 g (89.2%).

Synthesis of Octa(aminophenyl)silsesquioxane (OAPS)

Laine's method was followed to synthesize OAPS [27]. ONPS (10 g, 7.18 mmol.) and 10 wt% Pd/C (0.61 g 0.578 mmol.) were placed in a three-necked, round-bottomed flask fitted with a magnetic stirrer. A steady stream of nitrogen was passed continuously through the flask and freshly distilled THF (80 mL) and triethylamine (80 mL) were then added to the vessel. The resulting mixture was heated to 60 °C, followed by the gradual addition of 85% formic acid (10.4 mL, 0.23 mol.), which resulted in the evolution of CO_2. After the complete evolution of CO2, the solution separated into two layers was allowed to stand at 60 °C for 12 h. Then, the THF layer was isolated followed by adding a mixture of THF (50 mL) and water (50 mL) to the black residue and the resulting black suspension and THF layer were filtered through celite. Ethylacetate (50 mL) was added to the filtrate, which was washed with water and dried over anhydrous magnesium sulphate, before the organic layer was decanted and precipitated with hexane. The resulting precipitate of (octa(aminophenyl)silsesquioxane (Scheme 2) was filtered and dried in vacuum at 60 °C for 2 weeks. Yield: 6.9 g (76%).

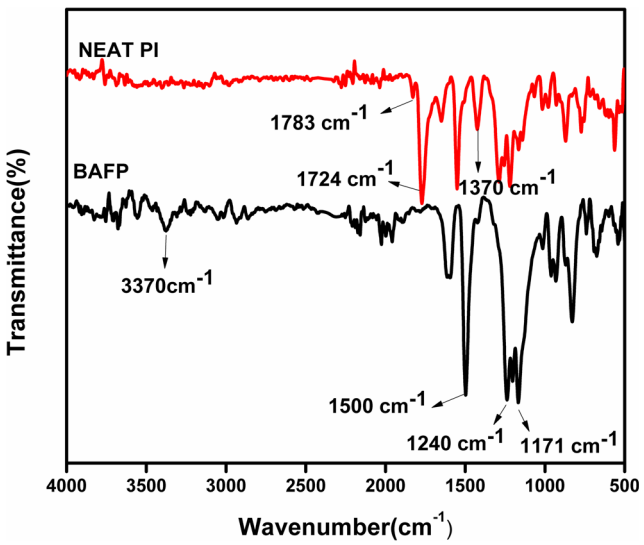

Fig. 1 FT-IR Spectra of BAFP diamine and neat PI

Preparation of OAPS-GO

Graphene oxide (GO) 0.5 g was dispersed in anhydrous NMP (10 mL), through sonication leading to disperse GO in solution uniformly. GO solution was then placed in a 100 mL three-necked flask, which was equipped with a magnetic stirrer, and a nitrogen inlet and outlet. Simultaneously, OAPS 4.34 g was dispersed in 40 mL of NMP through sonication, and the OAPS solution was also added to the three-necked flask reactor. The mixture was refluxed and stirred at 60 °C for 24 h in a nitrogen atmosphere, cooled to ambient

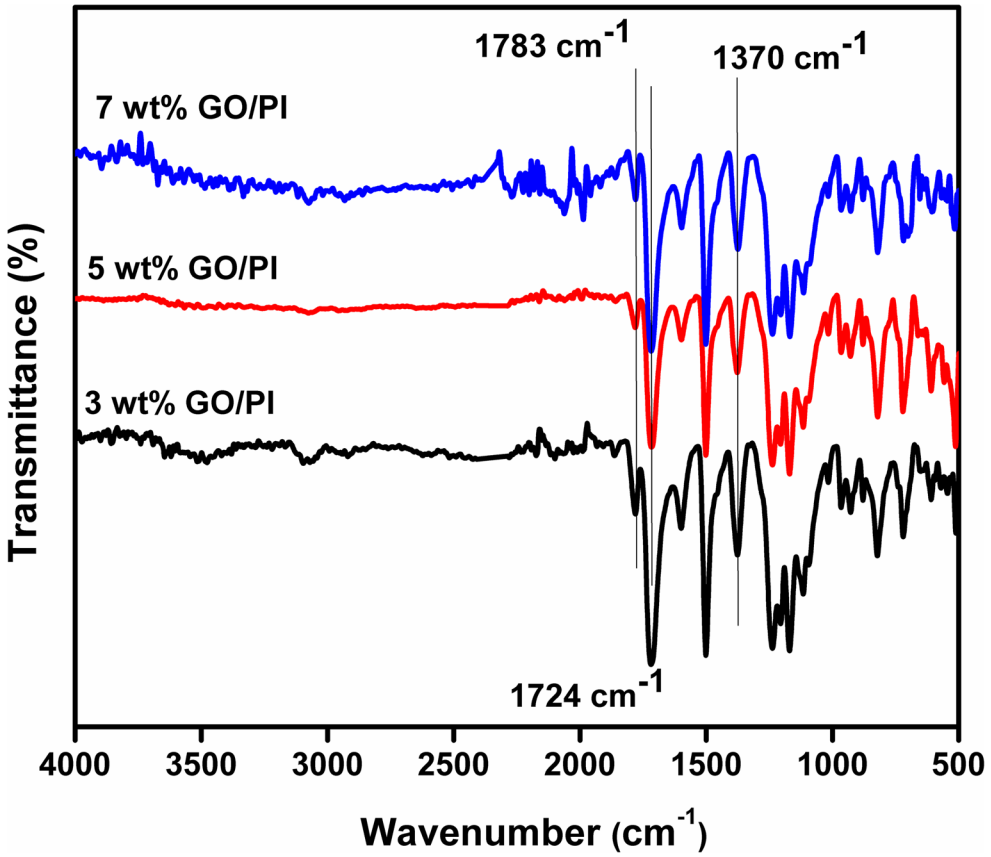

Fig. 2 FT-IR Spectra of GO/PI composites

temperature and filtered and washed with NMP and then the OAPS-functionalized GO (Scheme 3) referred to as OAPS-GO [28] collected and preserved for further use.

Preparation of neat PI, GO/PI, OAPS-GO/PI and OAPS/PI composites

The neat PI was prepared by the condensation of equimolar ratio of diamine BAFP (0.003 mol) and PMDA, using N-methyl-2-pyrrolidone (NMP) as the solvent. The solution of BAFP and PMDA in NMP has been purged with nitrogen (N_2) gas to remove the moisture and then the reaction mixture was stirred under N_2 atmosphere for 6 h at room temperature to form polyamic acid (PAA). Subsequently, the PAA was cast on a smooth glass substrate and thermally treated at 80 °C for 8 h, 200 °C for 2 h, and 300 °C for 2 h to obtain neat PI. The Schematic representation was also given in Scheme 4. Similar to the preparation of neat PI, the composites were also prepared with the addition of 3, 5 and 7 wt% of GO (Scheme 5), OAPS-GO (Scheme 6) and OAPS (Scheme 7) respectively.

Measurements

^{1}H and ^{13}C NMR spectra were recorded on a Bruker-400 NMR spectrometer (Bruker Corporation; massachusetts, USA). 5 mg of samples were ground with potassium bromide (KBr) powder and pelletized subsequently the Fourier transform infrared (FTIR) spectra of KBr pellets containing sample were obtained using a Bruker Tensor 27 FTIR spectrophotometer. Thermogravimetric analysis (TGA) of the polymer nanocomposites were carried out with an Exstar 6300 (Hitachi, Tokyo, Japan) at a heating rate of 10 °Cmin^{-1} under N_2 atmosphere. The surface overview of the composites was identified from FEI Quanta 200F (Oregon, USA) high-resolution scanning electron microscopy (HRSEM). Dielectric constant was determined by LCR meter (NumetriQ, PSM – 1735, UK). Contact angle measurements were obtained using a Ramehart Inc. goniometer with 5 μl of water as probe liquid.

Results and discussion

Structural elucidation

The molecular structure of BAFP was confirmed by ^{1}H and ^{13}C NMR spectrum. The obtained ^{1}H and ^{13}C NMR are illustrated in Figs. S3 and S4 respectively. In Fig. S3, the signals appearing from 6.59 to 6.92 ppm are assigned to six symmetric protons of aromatic ring and each proton is appearing as doublet. The signals appearing from 7.23 to 7.25 ppm are assigned to the

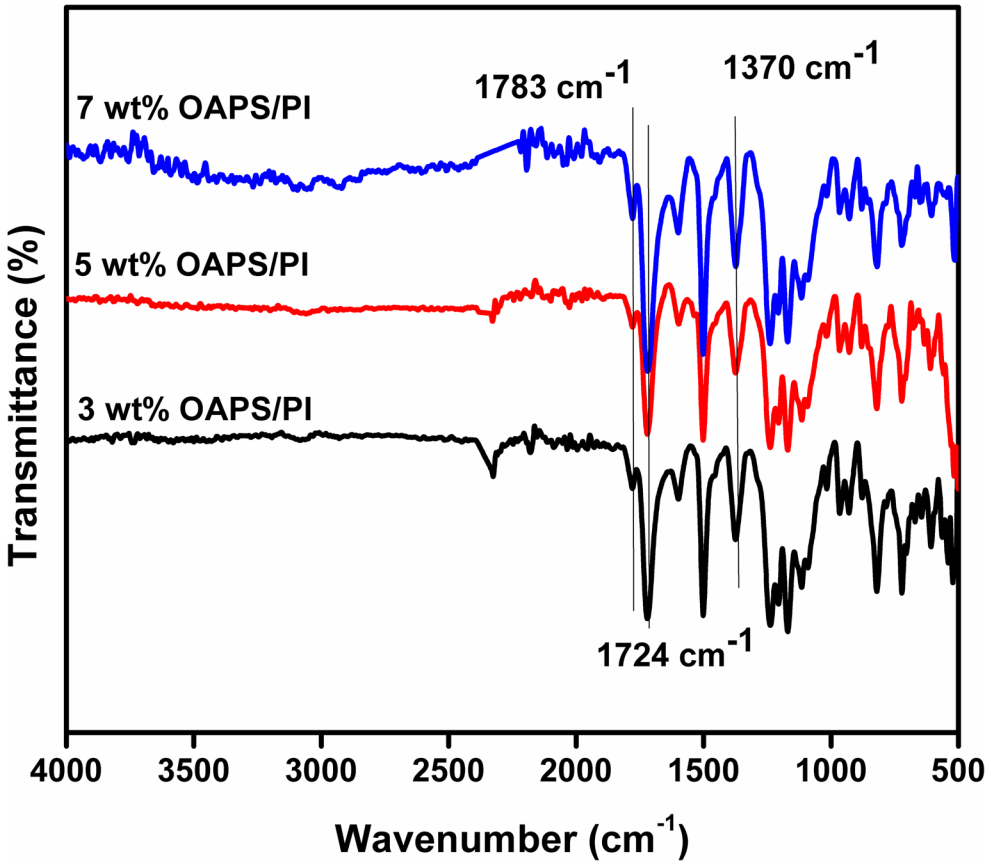

Fig. 3 FT-IR Spectra of OAPS/PI composites

two aromatic protons next to fluorine atoms. The peak associated for primary amine is appeared at 5.04 ppm which confirms the formation of diamine BAFP and occurrence of reduction. In addition to ^{1}H NMR, the formation of diamine was also confirmed by ^{13}C NMR (Fig. S4), the peaks appearing from 114.93 to 159.67 ppm are attributed to aromatic carbons. Moreover there is quartet at 125 ppm which is due to the coupling of hetero nuclear of ^{13}C and ^{19}F atoms which helps in reducing the value dielectric constant [29].

Figure 1 presents the FTIR spectra of the prepared BAFP and neat PI. The strong absorption band appeared at 3370 cm^{-1} (Fig. 1) corresponds to the N-H stretching of amino group, which supports results of NMR. Further, absorption bands appeared at 1240 and 1171 cm^{-1} are

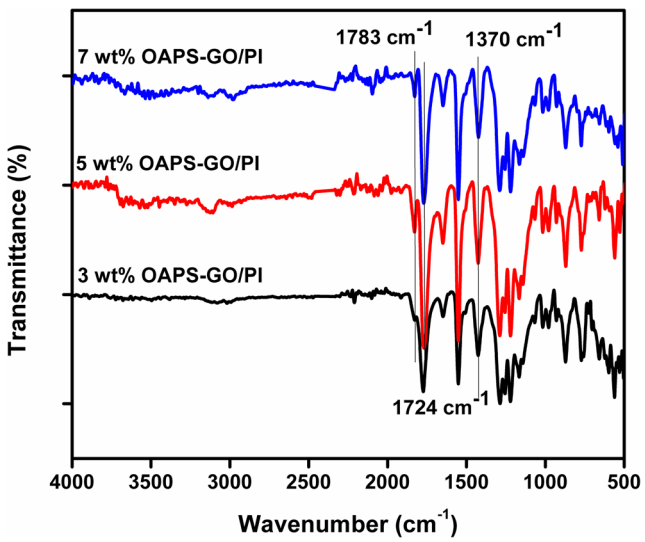

Fig. 4 FT-IR Spectra of OAPS-GO/PI composites

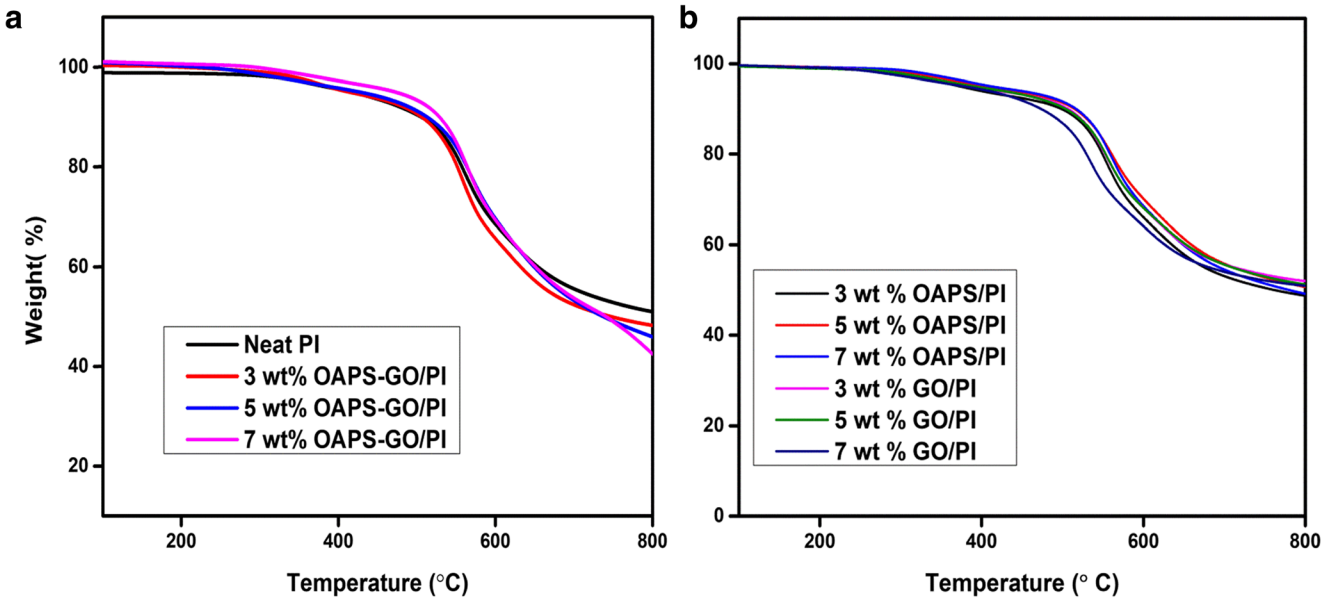

Fig. 5 TGA Spectra for Composites (**a**) Neat PI and OAPS-GO/PI composites (**b**) OAPS-GO/PI and GO/PI

attributed to C–O bond of ether linkage present in the BAFP. Further, the FTIR spectra of neat PI and composites shows no band related to amine at 3370 cm^{-1}, which confirms the formation of condensation reaction between the amine and anhydride. The new absorption bands appeared at 1783 cm^{-1} and 1370 cm^{-1} are attributed to the C=O unsymmetrical stretching and C-N stretching of imide groups. Further, the FTIR spectra of OAPS/PI, GO/PI and OAPS-GO/PI nanocomposites are shown in Figs. 2, 3 and 4 respectively. The absorption band at 1074 cm^{-1} in Figs. 3 and 4 are related to asymmetric Si-O-Si bonds present in POSS molecules, which confirms the presence of OAPS in the PI matrices. However, the peaks corresponding to Si-O-Si are not observed for the composites of GO reinforced PI (Figs. 2, 3 and 4).

Thermal properties

Figure 5a shows the thermal behaviour of neat PI and OAPS-GO/PI nanocomposites. Figure 5b shows the thermal behaviour of GO/PI and OAPS/PI nanocomposites. The thermal degradation temperature and char residue of the neat PI and composites are presented in Table 1. Initial degradation below 120 °C is associated with the removal of moisture. The thermal degradation pattern presented in Fig. 5a and b, indicate that the compound is significantly stable due to the formation of covalent bond between the reinforcements and the organic substituent's, hence, the degradations are limited over the temperature range of 200–500 °C [30, 31]. In Fig. 5a, OAPS-GO/PI composites exhibits comparatively lower thermal stability than that of neat PI. This is due to the formation of weak

Table 1 Thermal properties, Dielectric constant and water contact angle values of PI and PI composites

Sample	Degradation temperature T_{10} (°C)	Char yield (%) at 800 °C	LOI at 800 °C	Dielectric constant at 1 MHz	Water contact angle (θ)
Neat PI	497	54.8	39.4	3.3	95.7
3 wt% OAPS/PI	499	53.0	38.7	2.7	96.4
5 wt% OAPS/PI	515	55.8	39.8	2.5	99.3
7 wt% OAPS/PI	517	54.5	39.0	2.2	102.8
3 wt% GO/PI	507	55.6	39.7	2.8	91.7
5 wt% GO/PI	504	55.6	39.7	2.6	92.7
7 wt% GO/PI	473	54.0	39.1	2.3	94.4
3 wt% OAPS-GO/PI	506	52.3	38.4	2.6	93.3
5 wt% OAPS-GO/PI	513	53.2	38.7	2.4	97.8
7 wt% OAPS-GO/PI	528	53.6	38.9	2.1	107.4

physical attraction between the matrix and reinforcement, which in turn contributes to less thermal stability to the composites. Earlier, it was reported that the OAPS on the GO cage might undergone only hydrogen bonding, and decomposition of the low-molecular-weight compounds [32]. However, the earlier POSS reinforced polyimides systems are found to show enhanced thermal properties due to the direct attachment of matrix with the siloxane core of POSS [32]. Further, it is interesting to note that the similar patterns have been observed for the composites formed by individual reinforcement of OAPS and GO [33, 34].

The incorporation of OAPS individually into the polyimide system (Fig. 5b) showed remarkable improvements in thermal stability of PI. As the concentration increases, the degradation temperatures is retarded due to the presence of thermally stable cage structure of POSS reinforcement, strong aromatic backbone and fluorine moieties present in the polyimide system. Further, with respect to GO/PI composites (Fig. 3b), the degradation temperature follows similar trend as OAPS reinforced PI composites. As the concentration of GO increases the interfacial interaction between the polyimide and GO becomes higher in nature, which in turn contributes for the

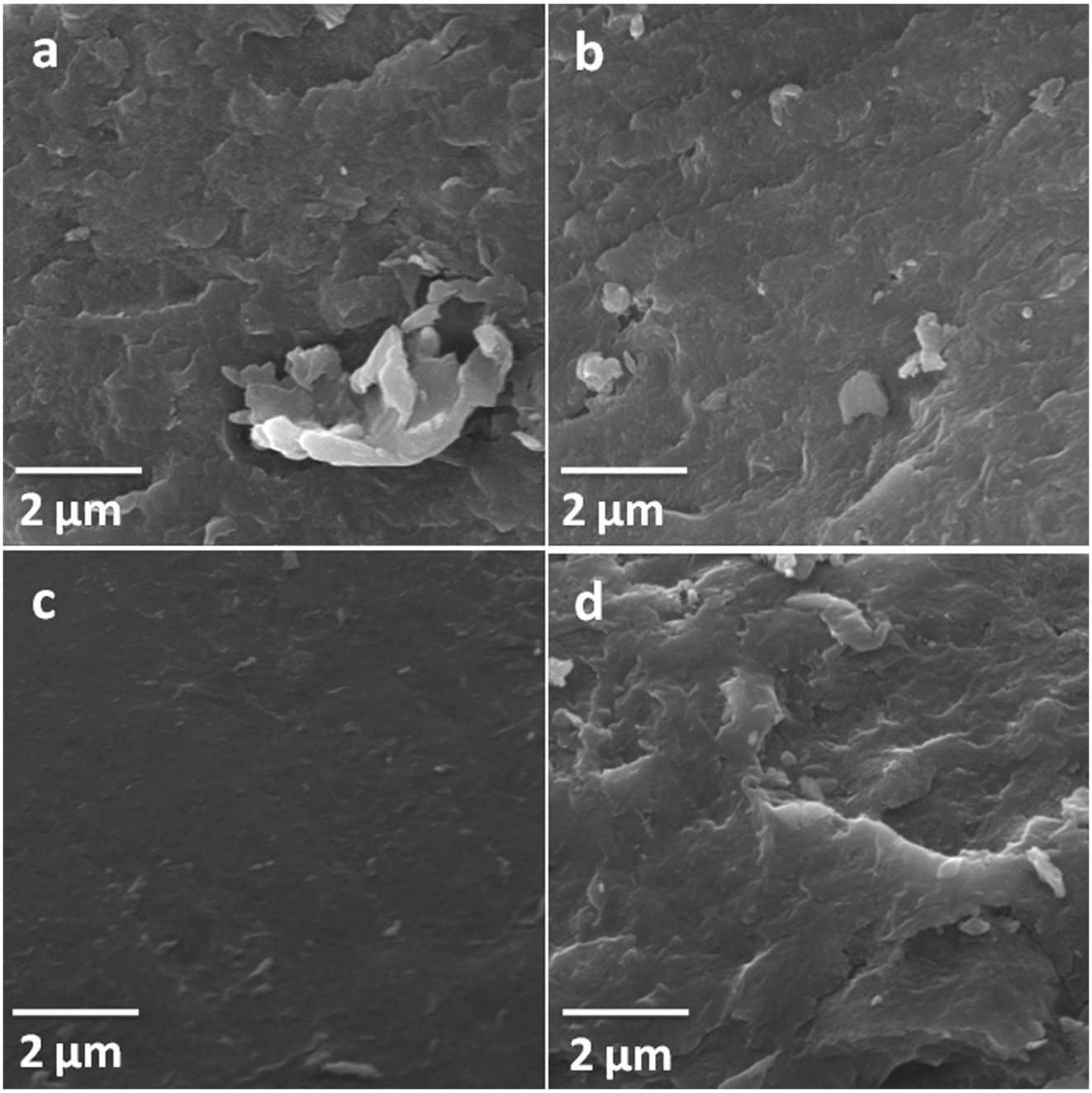

Fig. 6 SEM images of (**a**) Neat PI, (**b**)7 wt% GO/PI, (**c**)7 wt% OAPS/PI and (**d**) OAPS-GO/PI

enhanced thermal stability of the composites. The obtained results are in accordance with the previous reports [35–37].

Flame retardant behavior

The Limiting Oxygen Index (LOI) represents the lowest environmental oxygen content for sustaining a flame and it is used to quantify the flame retardancy of organic polymers. In the present study the flame retardant behaviour of neat polyimide and the different weight percentages of OAPS, GO, and OAPS-GO reinforced polyimide composites were analyzed using the char yield obtained from thermogravimetric analysis by substituting in Van Krevelen'sequation [38]. The LOI values calculated are presented in Table 1. LOI = 17.5 + 0.4 CR, where CR is the percentage char yield of polymer remaining at 800 °C. The LOI values obtained indicate that the polyimide composites developed using three different reinforcements possess an excellent flame retardant behaviour due to the formation of network structure between polymer and reinforcements and their inherent molecular structure. Thus, the developed OAPS/PI, GO/PI and OAPS-GO/PI hybrid composite materials can be effectively used as an efficient flame retardant material for different industrial applications.

Morphological properties

Figure 6a–d shows the morphology of neat PI, 7 wt% GO/PI, 7 wt% OAPS/PI and 7 wt% OAPS-GO/PI composites. The neat PI (Fig. 6a) shows tough fractured morphology, whereas 7 wt% GO incorporated PI exhibit rough layered morphology. This may be explained due to the random orientations of GO with the PI sheets in the polymer matrix with better

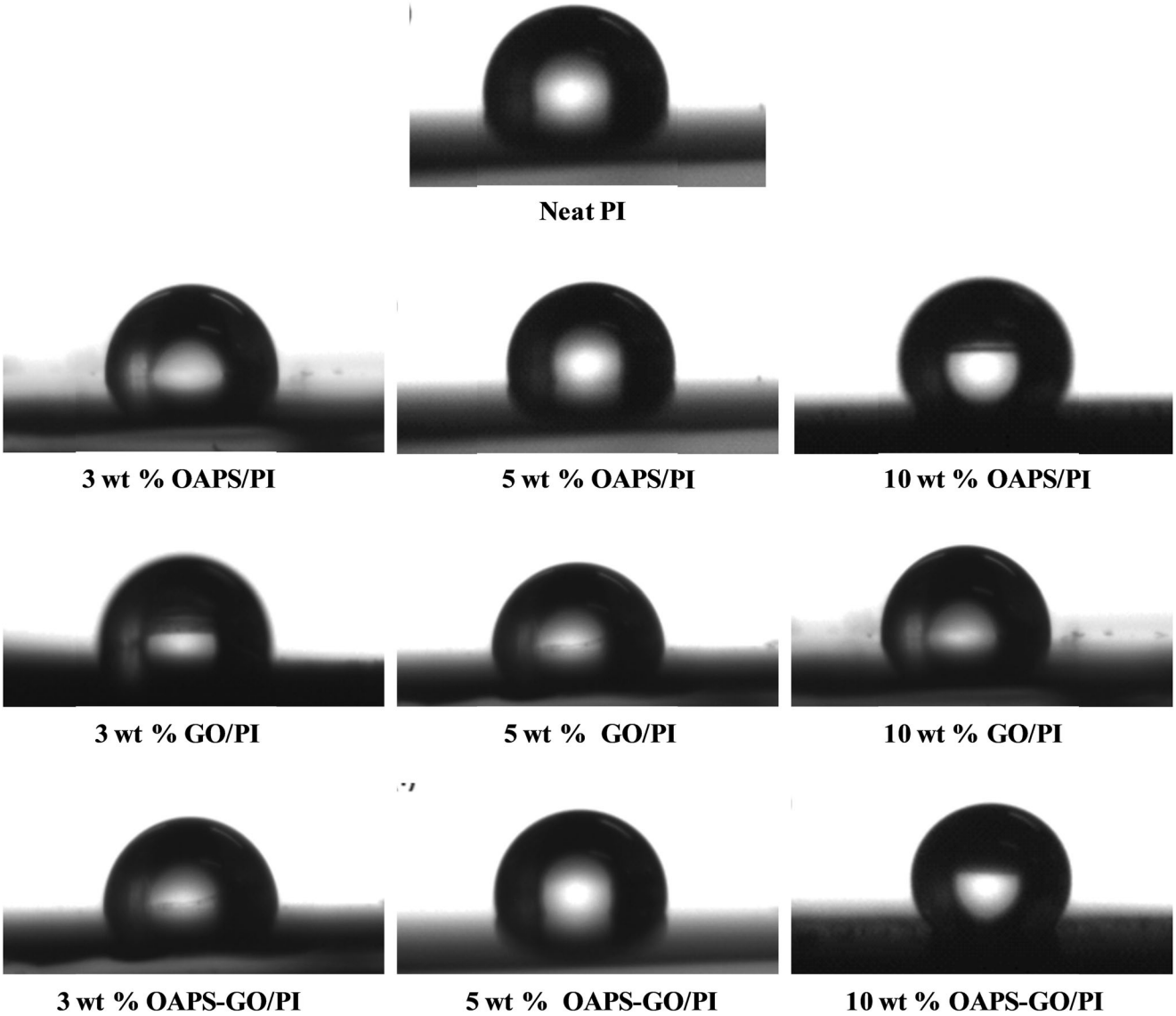

Fig. 7 Water contact angle images for neat PI and PI composites

homogeneity (Fig. 6b). In OAPS/PI system, there was no distinct phase separation, which infers that the OAPS reinforcement was homogeneously dispersed with PI matrix due to the formation of covalent bond between amino group and anhydride group (Fig. 6c). However, in OAPS-GO/PI (Fig. 6d) composites delivers homogeneous morphology which could be attributed due to the compatibility of OAPS-GO surface which influence in altering an important properties like dielectric constant and thermal stability.

Surface properties

The surface behaviour of neat polyimide and their composites were studied using contact angle measurement choosing water as probing liquid. The resulted images are presented in Fig. 7 and the obtained contact angle values are presented in Table 1. Compared to that of the neat PI, the results of composites tends to show increased value of contact angle. Thus, the 7% OAPS-GO reinforced PI composites shows the highest contact angle value of 107.4. This may be explained due to the enhanced hydrophobic behaviour and it is suggested that the developed composites can be used as an inter layer low-k dielectric materials in microelectronics industry for better performance.

Dielectric properties

The dielectric constant values of neat and varying weight percentages of GO/PI, OAPS/PI and OAPS-GO/PI nanocomposites are presented in Table 1. In OAPS-GO/PI composites (Fig. 8a), the nanoporous OAPS was grafted over the layered surfaces of GO, which forms OAPS-GO hybrid with more insulating behaviour. The presence of silica network over the GO retards lower polarization and in turn results in the formation of insulating behaviour to the resulted composites. Thus, the 7 wt% reinforced OAPS-GO/PI shows lowest dielectric constant (k = 2.1) than that of GO. Further, the insulating OAPS-GO present in the PI matrix restricts the electron mobility in the OAPS-GO/PI nanocomposites. Compared with GO/PI and OAPS/PI composite films, the OAPS-GO/PI composite films showed more reduction in the values of dielectric constant which could be attributed to the grafting of cage structured, nanoporous core (dielectric constant for air approx 1.0) of OAPS into the GO surface which could provide higher insulating properties than that of pristine GO sheets.

It was also observed that in GO/PI system (Fig. 8b), the dielectric constant values are decreased as the GO concentration increases from 3% to 7%. The decreasing trend was observed due to the presence of high density oxygen containing functional groups in GO which is considered as an electrically insulating material [39, 40]. Furthermore in GO/PI hybrids, the reduction in polarization takes place throughout the matrix and alters the structural arrangement due to the presence of GO content which

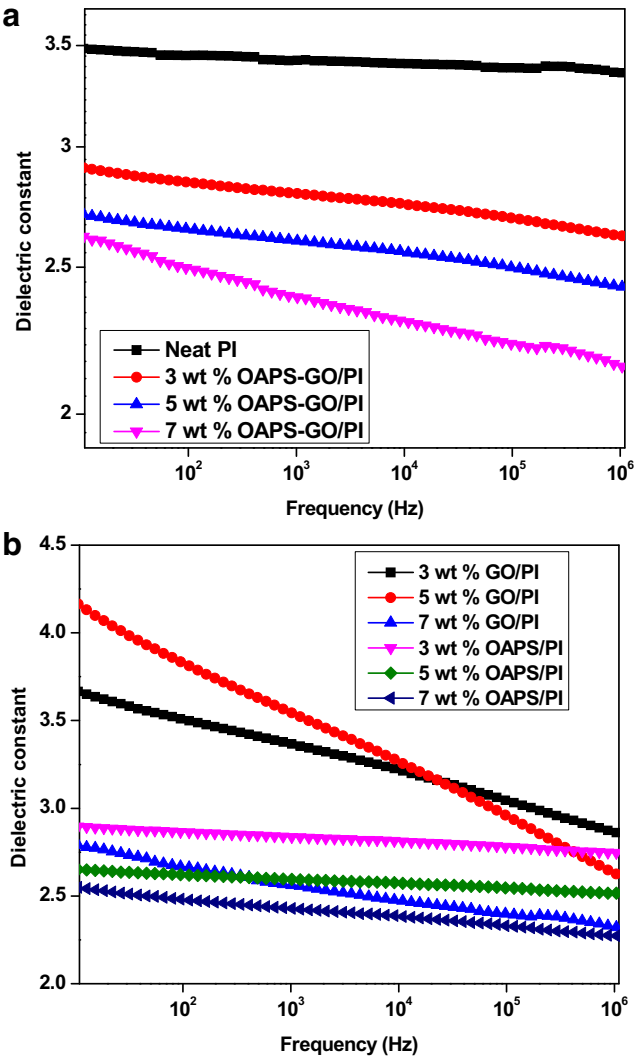

Fig. 8 Dielectric constant values for (**a**) Neat PI and OAPS-GO/PI composites, (**b**). Dielectric constant for GO/PI and OAPS/PI composites

in turn resulted in lower dielectric constant values. In addition, the formation of carbon - oxygen bonds on the GO surface and the modification of sp^2 hybridised carbon atoms in graphite to sp^3 carbon atoms in GO and the insertion of air/vacuum between the distinct layered structure are the main reasons for the less polarization behaviour of GO/PI nanocomposites.

Further in the case of OAPS/PI system (Table 1 and Fig. 8b), the OAPS incorporated PI has lower values of dielectric constant than that of structurally modified PI. The reduction in the value of dielectric constant was depends on the OAPS concentration. An increase in OAPS concentration into PI decreases the dipole–dipole interactions in the resulting nanocomposites. This is due to the presence of nanoporosity in the core of the OAPS molecules exhibiting a large free volume, and the less polar nature of the resulting hybrid nanocomposites [41].

The dielectric loss tangent of OAPS-GO/PI and GO/PI&OAPS/PI nanocomposites are presented in Figs. S7 and S8 respectively. The dielectric loss value of materials are

generally obtained from factors such as direct current(DC) conduction, space charge migration (interfacial polarization contribution) and the movement of molecular dipoles(dipole loss) [42, 43]. Data from dielectric loss studies indicate that OAPS-GO/PI composites system possesses lower value of dielectric loss when compared to those of OAPS/PI and GO/PI systems. Due to the grafting of cage structures with nanoporous core of OAPS over the GO, which form more insulation layer on the surface. Thus, the polarization of surfaces functional groups are completely retarded which could provide higher insulating properties than that of resulted composites.

Conclusion

In the present work, three types of hybrid composites have been developed using varying weight percentages of GO, OAPS and OAPS-GO reinforcements and were characterised by different analytical techniques. Results obtained from dielectric studies, it was observed that the OAPS-GO /PI hybrid composites possesses the lowest value of dielectric constant when compared with those of GO/PI and OAPS/PI composite films, due to the presence of the cage structured OAPS with a nanoporous core (dielectric constant of air is approx 1.0) was grafted onto the GO surface which enhances the insulating properties when compared to that of pristine GO sheets. The data obtained from thermal, morphological and dielectric studies indicated that among three different PI composites systems such as GO/PI, OAPS-GO/PI and OAPS/PI, OAPS-GO/PI system exhibited a substantially improved thermal stability, hydrophobic behaviour and dielectric properties. From the results obtained, it is suggested that PI/OAPS-GO hybrid composite system can be utilized in the fabrication of microelectronic devices for high performance applications with improved longevity.

References

1. Sasikumar R, Ariraman M, Alagar M (2014) Design of lamellar structured POSS/BPZ polybenzoxazine nanocomposites as the novel class of ultra low k dielectric material. RSC Adv 4: 19127–19136
2. Maier G (2001) Low dielectric constant polymers for microelectronics. Prog Polym Sci 26:3–65
3. Feger C, Franke H (1996) Polyimides in high-performance electronics packaging and optoelectronic applications. In: Ghosh MK, Mittal KL (eds) Polyimides fundamentals and applications. Marcel Decker, New York, pp 759–814
4. Yu P, Wang Y, Yu J, Zhu J, Hu Z (2018) Influence of different ratios of a-ODPA/a-BPDA on the properties of phenylethynyl terminated polyimide. J Polym Res 25(5):110
5. Muruganand S, Varayandass, Sa K, Mangalaraj D, Vijayan TM (2001) Dielectric and conduction properties of pure polyimide films. Polym Int 50:1089–1094
6. Kuntman A, Kuntman H (2000) A study on dielectric properties of a new polyimide film suitable for interlayer dielectric material in microelectronics applications. Microelectron J 31:629–634
7. Gunasekaran SG, Rajakumar K, Alagar M, Dharmendirakumar M (2014) Siloxane core dianhydride modified ether linked cyclohexyl diamine based multi-walled carbon nanotube reinforced polyimide (MWCNT/PI) nanocomposites. J Polym Res 21(1):342
8. Zhang Y, Liu J, Wu X, Guo C, Qu L, Zhang X (2018) Trisilanolphenyl-POSS nano-hybrid poly (biphenyl dianhydride-p-phenylenediamine) polyimide composite films: miscibility and structure-property relationship. J Polym Res 25(6):139
9. Ghosh MK, Mittal KL (1996) Polyimide: fundamentals and applications. Marcel Dekker, New York
10. Geim A, Novoselov K (2007) The rise of grapheme. Nat Mater 6: 183–191
11. Devaraju S, Vengatesan MR, Alagar M (2011) Studies on thermal and dielectric properties of ether linked cyclohexyl diamine (ELCD)-based polyimide POSS nanocomposites (POSS-PI). High Perform Polym 23:99–111
12. Kurinchyselvan S, Sasikumar R, Ariraman M, Gomathipriya P, Alagar M (2016) Low dielectric behavior of amine functionalized MCM-41 reinforced polyimide nanocomposites. High Perform Polym 28(7):842–853
13. Husamelden E, Fan H (2019) Fluorinated functionalization of graphene oxide and its role as a reinforcement in epoxy composites. J Polym Res 26(2):42
14. Kim H, Abdala AA, Macosko CW (2010) Graphene/polymer nanocomposites, macromolecules, macromolecules, vol 43, pp 6515–6530
15. Rafiee MA, Rafiee ZJ, Wang H, Song ZZ, Yu Koratkar N (2009) Enhanced mechanical properties of nanocomposites at low graphene content. ACS Nano 3:3884–3890
16. Verdejo R, Bernal MM, Romasanta LJ, Lopez-Manchado MA (2011) Graphene filled polymer nanocomposites. J Mater Chem 21:3301–3310
17. Zhao X, Zhang Q, Chen D, Lu P (2010) Enhanced mechanical properties of graphene-based poly (vinyl alcohol) composites. Macromolecules 43:2357–2363
18. Hontoria-Lucas C, Lopez-Peinado A, Lopez-Gonzalez JD, Rojas-Cervantes M, Martin-Aranda R (1995) Study of oxygen-containing groups in a series of graphite oxides: physical and chemical characterization. Carbon 33:585–1592
19. Kotov NA, Dekany I, Fendler JH (1996) Ultrathin graphite oxide-polyelectrolyte composites prepared by self-assembly: transition between conductive and non-conductive states. Adv Mater 8:637–641
20. Szabo T, Szeri A, Dekany I (2005) Composite graphitic nanolayers prepared by self-assembly between finely dispersed graphite oxide and a cationic polymer. Carbon 43:87–94
21. Sasikumar R, Alagar M (2015) Dielectric and thermal behaviours of POSS reinforced polyurethane based polybenzoxazine nanocomposites. RSC Adv 5:33008–33015
22. Wahab MA, Mya KY, He C (2008) Synthesis ,morphology and properties of hydroxyl terminated-POSS/polyimide low-k nanocomposite films. J Polym Sci A Polym Chem 46:5887–5896
23. Kuo SW, Chang FC (2011) POSS related polymer nanocomposites. Prog Polym Sci 36:1649–1696
24. Zhang W, Müller AHE (2013) Architecture self-assembly and properties of well-defined hybrid polymers based on Polyhedral Oligomeric Silsequioxane (POSS). Prog Polym Sci 38:1121–1162
25. Liang K, Li G, Toghiani H, Koo JH, Pittman CU (2005) Cyanate ester/ Polyhedral Oligomeric Silsesquioxane (POSS) nanocomposites:synthesis and characterization. Chem Mater 18:301–312

26. Lee YJ, Huang JM, Kuo SW, Lu JS, Chang FC (2005) Polyimide and polyhedral oligomeric Silsesquioxane nanocomposites for low-dielectric applications. Polymer 46:173–181
27. Laine RM (2005) Nanobuilding blocks based on the [OSiO1-5]x (x=6,8,10) octasilsesquioxanes. J Mater Chem 35:3725–3744
28. Liao WH, Yang SY, Hsiao ST, Wang YS, Li SM, Ma CCM, Tien HW, Zeng SJ (2014). ACS Appl Mater Interfaces 6:15802–15812
29. Hariharan R, Sarojadevi M (2007) Synthesis and characterization of organo-soluble fluorinated polyimides. Polym Int 56:22–31
30. Govindaraj B, Sundararajan P, Sarojadevi M (2012) Synthesis and characterization of polyimide/polyhedral oligomeric silsesquioxane nanocomposites containing quinolyl moiety. Polym Int 61:1344–1352
31. Figueiredo JL, Pereira MFR, Freitas MMA, Orfao JJM (1999) Modification of the surface chemistry of activated carbons. Carbon 37:1379–1389
32. Ye YS, Yen YC, Chen WY, Cheng CC, Chang FC (2008) A simple approach toward low-dielectric polyimide nanocomposites: blending the polyimide precursor with a fluorinated polyhedral oligomeric silsesquioxane. J Polym Sci A Polym Chem 46(18):6296–6304
33. Mohamed M, Kuo S (2019) Functional polyimide/polyhedral oligomeric silsesquioxane nanocomposites. Polymers 11(1):26
34. Mohamed MG, Kuo SW (2019) Functional silica and carbon nanocomposites based on polybenzoxazines. Macromol Chem Phys 220(1):1800306
35. Xue Y, Liu Y, Lu F, Qu J, Chen H, Dai L (2012) Functionalization of graphene oxide with Polyhedral Oligomeric Silsesquioxane (POSS) for multifunctional applications. J Phys Chem Lett 3: 1607–1612
36. Teng CC, Ma CCM, Lu CH, Yang SY, Lee SH, Hsiao MC, Yen MY, Chiou KC, Lee TM (2011) Thermal conductivity and structure of non-covalent functionalized graphene/ epoxy composites. Carbon 49:5107–5116
37. Liao WH, Tien HW, Hsiao ST, Li SM, Wang YS, Huang YL, Yang SY, Ma CCM, Wu YF (2013) Effects of multiwalled carbon nanotubes functionalization on the morphology and mechanical and thermal properties of carbon fiber/vinyl Ester composites. ACS Appl Mater Interfaces 5:3975–3982
38. Van Krevelen DW (1975) Some basic aspects of flame resistance of polymeric materials. Polymer 16:615–620
39. Dreyer DR, Park S, Bielawski CW, Ruoff RS (2010) The chemistry of graphene oxide. Chem Soc Rev 39:228–240
40. Wang Z, Nelson JK, Hillborg H, Zhao S, Schadler LS (2012) Graphene oxide filled nanocomposite with novel electrical and dielectric properties. Adv Mater 24:3134–3137
41. Huang J, Lim PC, Shen L, Pallathadka PK, Zeng K, He C (2005) Cubic silsesquioxane–polyimide nanocomposites with improved thermomechanical and dielectric properties. Acta Mater 53:2395–2404
42. Purushothaman R, Bilal IM, Palanichamy M (2011) Effect of chemical structure of aromatic dianhydrides on the thermal, mechanical and electrical properties of their terpolyimides with 4, 4′-oxydianiline. J Polym Res 18(6):1597–1604
43. Jonsher AK (1977) The 'universal dielectric response. Nature 267: 673–679